
SPHERE: Spherical partitioning for large-scale routing optimization

Robert Fabian Lindermann¹ Paul-Niklas Ken Kandora¹ Simon Caspar Zeller¹ Adrian Asmund Fessler¹
Steffen Rebennack¹

¹Institute for Operations Research, Karlsruhe Institute of Technology, Karlsruhe, Germany, {paul-niklas.kandora, simon.zeller, steffen.rebennack}@kit.edu, {robert.lindermann, adrian.fessler}@student.kit.edu

Abstract

We study shortest-path routing in large weighted, undirected graphs, where expanding search frontiers raise time and memory costs for exact solvers. We propose *SPHERE*, a query-aware partitioning heuristic that adaptively splits the problem by identifying *source-target* (s - t) overlaps of hop-distance spheres. Selecting an anchor node a within this overlap partitions the task into independent induced subgraphs for $s \rightarrow a$ and $a \rightarrow t$, each restricted to its own induced subgraph. If resulting subgraphs remain large, the procedure recurses on that specific subgraph. We provide a formal guarantee that by using the partition cut within the shared overlap, the resulting subpaths preserve feasibility, thereby avoiding the need for boundary repair. Furthermore, *SPHERE* acts as a solver-agnostic framework that naturally exposes parallelism across subproblems. On million-scale road networks, *SPHERE* achieves faster runtimes and smaller optimality gaps than contemporary state-of-the-art partitioning and community-based routing pipelines. Crucially, it also substantially mitigates heavy-tail runtime outliers suffered by standard exact methods, yielding highly stable and predictable execution times across varying queries.

1 INTRODUCTION

Point-to-point routing in large weighted, undirected graphs is a canonical problem in operations research, one that emerged alongside the field's inception. Exact label-setting or label-correcting methods (e.g., Dijkstra) can certify optimality [Dijkstra, 1959], but their search frontiers grow quickly on large networks and become memory- and time-intensive. Graph partitioning methods (e.g., Kernighan-Lin, multilevel partitioning/METIS, spectral cuts) reduce prob-

lem size by cutting the graph into parts [Kernighan and Lin, 1970, Karypis and Kumar, 1998, Shi and Malik, 2000], yet cuts chosen without regard to a specific query (s, t) can intersect narrow passages that many feasible s - t routes must use, which can exclude high-quality routes or require costly boundary repair. Bidirectional search reduces depth by growing frontiers from s and t [Nicholson, 1966, Pohl, 1969, Kaindl and Kainz, 1997, Holte et al., 2016], but still explores a single coupled state space and may expand many partial routes on large graphs. For completeness, we note that while feasibility for unconstrained shortest paths is trivial on connected graphs, constrained variants (e.g., resource- or budget-limited paths) are NP-hard; our focus here is the unconstrained case with nonnegative weights, which admits an optimal solution via Dijkstra's algorithm [Dijkstra, 1959].

We propose *SPHERE*, a query-aware source-target partitioning heuristic that aligns computation directly with the s - t geometry. Let $S_R(s)$ and $S_R(t)$ denote *hop-distance spheres* centered around s and t . *SPHERE* initializes a radius tuple (R_s, R_t) large enough to guarantee a nonempty overlap; $S_{R_s}(s) \cap S_{R_t}(t) \neq \emptyset$. *SPHERE* then applies a monotone *decrement* rule to systematically shrink the radii, maintaining a balanced scale ($|R_s - R_t| \leq 1$) until reaching the *minimal balanced pair* which refers to the situation where any further valid reduction of either radius would leave the intersection empty.

From this minimal overlap, the algorithm selects an anchor node $a \in S_{R_s}(s) \cap S_{R_t}(t)$. This anchor effectively splits the original source-target pair s - t into two independent subproblems, $s \rightarrow a$ and $a \rightarrow t$, which are then solved on their respective induced subgraphs subject to a tunable bound. This tunable bound is a bound that limits the maximum hop-radius of a subproblem which we refer to as R_{\max} . If a resulting subproblem still exceeds this cap, the procedure simply recurses on its induced subgraph.

Crucially, because the anchor a sits inside the shared overlap, it exists in both induced subgraphs simultaneously. This guarantees that the local $s \rightarrow a$ path and the local $a \rightarrow t$ path will physically connect at a , seamlessly forming a con-

tinuous, valid $s-t$ route without requiring any secondary algorithms to repair broken links across the cut. Finally, *SPHERE* is solver-agnostic and generates independent subproblems that can be executed in parallel. We make the following contributions:

1. **Query-Aware Geometric Partitioning:** We introduce a heuristic that adaptively partitions the graph based on the specific $s-t$ geometry by cutting inside the last nonempty overlap of hop-distance spheres. This ensures that each part preserves local connectivity and can be rejoined at an anchor node without the need for costly boundary repair.
2. **Theoretical Guarantees:** We formalize the spherical partitioning algorithm and prove that our cut placement intrinsically preserves global route feasibility. Furthermore, for unweighted, undirected graphs we establish theoretical conditions under which the recursive application of this partition guarantees a globally optimal shortest path.
3. **Solver-Agnostic Parallel Execution:** The subproblems generated by *SPHERE* are completely independent induced subgraphs. This allows the subproblems to be solved in parallel. Because *SPHERE* generates standard graphs, start nodes, and anchor nodes to the downstream solver, it is completely solver-agnostic. Any off-the-shelf routing algorithm (e.g. Dijkstra) can be used to compute local paths without the need to adjust the solver’s underlying structure.
4. **Empirical validation.** On large-scale networks with over a million nodes and edges, *SPHERE* achieves faster runtimes and smaller optimality gaps than other state-of-the-art $s-t$ routing approaches. Crucially, it also substantially mitigates heavy-tail runtime slowdowns observed in standard methods, resulting in highly stable and predictable execution times across varying queries.

2 MOTIVATION

Algorithms for routing at scale inherently struggle to balance search space complexity, route exactness, and practical scalability [Bast et al., 2016]. Building on these established challenges, routing at scale must meet three criteria simultaneously: control per-instance complexity, guarantee route feasibility, and enable parallel execution with standard solvers. Existing tools typically sacrifice at least one of these:

Labeling methods preserve feasibility, but generate a *combinatorial explosion* of partial routes due to the complexity of the topology of large graphs [Feillet et al., 2004, Irnich and Desaulniers, 2005]. Graph partitioners such as [Kernighan and Lin, 1970, Karypis and Kumar, 1998, Shi and Malik, 2000] successfully control instance size, but their static

boundaries ignore the specific s and t locations. This risks cutting across critical bottlenecks and losing *feasible routes*. Bidirectional search [Nicholson, 1966, Pohl, 1969, Kaindl and Kainz, 1997, Holte et al., 2016] reduces depth but explores a single coupled state space that cannot be partitioned into *independent pieces*, making it difficult to enforce parallelism. While static partitioning methods like Corridor routing could theoretically be parallelized, they often require shared boundary information or synchronization across a global quotient graph to ensure path consistency. In contrast, *SPHERE*’s subproblems are mathematically independent by construction. Because the anchor node a is guaranteed to exist in both induced subgraphs, no inter-process communication or boundary repair is required during the solve phase, allowing for true solver-agnostic parallel execution.

In comparison, *SPHERE* avoids *combinatorial explosion* by bounding subproblems within hop-distance spheres, strictly limited by a tunable bound (R_{\max}). Additionally, *SPHERE* cuts exclusively inside the shared $s-t$ overlap and preserves local connectivity and guarantees a *feasible route* upon concatenation without any need for boundary repair. The induced subgraphs generated by *SPHERE* naturally expose parallel execution and act as a solver-agnostic framework, allowing practitioners to drop-in any trusted downstream optimizer, from exact Mixed-Integer Programming (MIP) to strong metaheuristics [Pisinger and Ropke, 2007, Vidal, 2022], without modification.

In short, *SPHERE* offers a partition strategy that controls complexity, preserves feasibility, and exposes natural parallelism while remaining compatible with the solvers practitioners already trust.

3 RELATED WORK

Point-to-point routing on large weighted graphs has been studied from several perspectives. Classical exact methods such as label-setting and label-correcting algorithms (e.g., Dijkstra) can guarantee global optimality on connected graphs with nonnegative weights [Dijkstra, 1959]. Dynamic-programming and labeling variants extend this to richer settings and can certify optimality, but they often face an explosion in the number of variables on large graphs [Feillet et al., 2004, Irnich and Desaulniers, 2005]. Approximation schemes [Hassin, 1992] exist, trading accuracy for speed, yet these techniques operate on the full graph and therefore do not reduce the instance size before the optimization.

3.1 GRAPH PARTITIONING AND PARALLEL SOLVERS

Graph partitioning offers a complementary idea: simplify the problem by splitting the graph, a strategy specifically suited for large-scale routing. Kernighan-Lin improves an

initial cut by greedy node swaps to reduce the number of edges crossing between parts while keeping parts balanced [Kernighan and Lin, 1970]. Multilevel schemes such as METIS repeatedly coarsen the graph, compute a cut on the coarse instance, and refine it during uncoarsening, which gives strong scalability in practice [Karypis and Kumar, 1998]. In routing pipelines, these partitions, along with community-based heuristics like the Louvain method, are often used to build a *quotient graph* for a coarse path or corridor that is later refined within parts [Blondel et al., 2008]. A limitation of all such methods is that the cut is chosen without regard to the specific start-target pair (s, t) , so the boundary can lie across a narrow passage that every feasible s - t path must use. Once this happens, the coarse or restricted routing stage may miss or degrade the necessary connection leading to potentially infeasible routes.

Parallel computation for shortest-path problems has also been studied to accelerate routing. For instance, Rozhoň et al. [2023] analyze parallel Breadth-First Search and approximate distances within subgraphs. However, this approach is mainly theoretically analyzed.

3.2 MACHINE LEARNING AND DEEP LEARNING-BASED APPROACHES

Recent advancements in neural combinatorial optimization have introduced Deep Learning models capable of solving complex routing tasks. Notable examples include Policy Optimization with Multiple Optima (POMO) [Kwon et al., 2020] and Multi-Task Vehicle Routing Solver with Mixture-of-Experts (MvMOE) [Zhou et al., 2024]. These neural solvers are primarily designed for distribution-trained variants of the Traveling Salesperson Problem (TSP) and Vehicle Routing Problem (VRP). Those methods operate effectively on small to medium-scale graphs.

3.3 BIDIRECTIONAL SEARCH

Bidirectional search reduces search depth by expanding frontiers from both ends and meeting near the middle [Nicholson, 1966, Pohl, 1969, Kaindl and Kainz, 1997]. The MM algorithm of Holte et al. [2016] provides a priority rule that ensures expansions do not go beyond the midpoint of the optimal solution. These methods improve exploration efficiency but still operate within a single coupled search space and do not produce small, independent instances. In large graphs this can still generate many partial routes, and unlike partition-based methods, they do not offer a straightforward path to parallel, solver-agnostic execution.

4 SPHERICAL PARTITIONING

4.1 SPHERICAL SUBGRAPHS

We begin by formalizing the local "window" around a node using hop-based distance. Throughout this work, let $G = (V, E)$ denote a finite, connected, and undirected graph with positive edge weights. Unless otherwise specified, we measure distance in *hops* (unweighted shortest path), though our formulations remain valid for weighted shortest-path distances. For a comprehensive summary of the mathematical notation used in this paper, please refer to Appendix A.1.

Definition 4.1 (Spheres) For $R \in \mathbb{N}$ and a reference node $\tilde{v} \in V$, the (closed) sphere is

$$S_R(\tilde{v}) := \{v \in V : d_G(\tilde{v}, v) \leq R\} \subseteq V,$$

where $d_G(\tilde{v}, v)$ is the unweighted shortest path distance between \tilde{v} and v .

Two standard subgraphs provide complementary local views of G on the node set $S_R(\tilde{v})$.

Definition 4.2 (Spherical subgraph) The spherical subgraph is defined as $G_R^{\text{SP}}(\tilde{v}) := (V_R(\tilde{v}), E_R^{\text{SP}}(\tilde{v}))$ with $V_R(\tilde{v}) := S_R(\tilde{v})$ and

$$E_R^{\text{SP}}(\tilde{v}) := \left\{ \{i, j\} \in E : d_G(\tilde{v}, i) \leq R, d_G(\tilde{v}, j) \leq R, \right. \\ \left. |d_G(\tilde{v}, i) - d_G(\tilde{v}, j)| = 1 \right\}.$$

Thus, $E_R^{\text{SP}}(\tilde{v})$ contains exactly those edges inside the sphere that connect consecutive distance layers and therefore lie on shortest paths from \tilde{v} .

Definition 4.3 (Induced spherical subgraph) The induced spherical subgraph, $G_R^{\text{IND}}(\tilde{v}) := (V_R(\tilde{v}), E_R^{\text{IND}}(\tilde{v}))$ is defined with $V_R(\tilde{v}) := S_R(\tilde{v})$ and

$$E_R^{\text{IND}}(\tilde{v}) := \{\{i, j\} \in E : i, j \in S_R(\tilde{v})\},$$

where $E_R^{\text{IND}}(\tilde{v})$ can be viewed as the edge-closure of the vertex set $S_R(\tilde{v})$, in the sense that all edges of G with both endpoints in $S_R(\tilde{v})$ are retained.

Clearly $E_R^{\text{SP}}(\tilde{v}) \subseteq E_R^{\text{IND}}(\tilde{v})$: the spherical subgraph preserves shortest-path connectivity to the center, while the induced version preserves all *local* connectivity.

4.2 PARTITION CUT

With these geometric building blocks established, we now align these local windows to a specific query (s, t) .

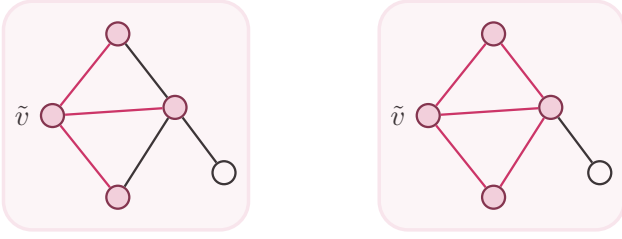
(a) $G_R^{\text{sp}}(\tilde{v})$ (b) $G_R^{\text{ind}}(\tilde{v})$ 

Figure 1: **Two local views on $S_R(\tilde{v})$.** Left: spherical subgraph. Right: induced subgraph.

Definition 4.4 For radii $(R_s, R_t) \in \mathbb{N}^2$, define the overlap as

$$O(R_s, R_t) := S_{R_s}(s) \cap S_{R_t}(t).$$

In order to identify a precise splitting point, we control how the radii evolve from their initial state to a minimal configuration. This necessitates defining the properties of *decrement rules*, which systematically shrink the search space.

Definition 4.5 (Decrement rule) A decrement rule

$$\text{decr}u : \mathbb{N}^2 \rightarrow \mathbb{N}^2$$

is a map that is monotone in the lexicographic order, i.e.,

$$(x_1, x_2) \leq_{\text{lex}} (y_1, y_2) \iff x_1 < y_1, \\ \text{or } (x_1 = y_1 \text{ and } x_2 \leq y_2).$$

and never increases any coordinate.

Example 4.6 (monotone decrement) A standard rule that satisfies these properties is one that prioritizes shrinking the larger sphere to keep the search balanced:

$$\text{decr}u(R_s, R_t) = \begin{cases} (R_s - 1, R_t), & R_s \geq R_t, \\ (R_s, R_t - 1), & \text{otherwise.} \end{cases}$$

This rule ensures the radii remain balanced ($|R_s - R_t| \leq 1$) throughout the process. If $(R_s, R_t) \leq_{\text{lex}} (R'_s, R'_t)$, the smaller pair cannot "overtake" the larger one, preserving the order of operations.

We make this procedure operational by defining two auxiliary rules for initialization and anchor selection:

Definition 4.7 (Starting rule) A starting rule

$$\text{star}u : V \times V \rightarrow \mathbb{N}^2$$

returns (R_s^0, R_t^0) with nonempty overlap $O(R_s^0, R_t^0) \neq \emptyset$ (e.g., $R_s^0 + R_t^0 \geq d_G(s, t)$); a stronger but safe choice is $S_{R_s^0}(s) \cup S_{R_t^0}(t) = V$.

Definition 4.8 (Anchor rule) An anchor rule

$$\text{anru} : \mathcal{P}(V) \rightarrow V$$

selects $a \in O(R_s, R_t)$ (e.g., uniform random).

The starting rule for initialization (Definition 4.7), decrement rule for shrinking (Definition 4.5) and anchor rule for selecting the split point (Definition 4.8), together define Algorithm 1, which we refer to as the *Partition cut*.

Algorithm 1 Partition cut

Require: graph $G = (V, E)$, terminals (s, t) , rules (staru, decru, anru)
Ensure: radii (\bar{R}_s, \bar{R}_t) , overlap O , anchor a

- 1: $(R_s, R_t) \leftarrow \text{star}u(s, t)$
- 2: **while** $O(R_s, R_t) \neq \emptyset$
- 3: $(\bar{R}_s, \bar{R}_t) \leftarrow (R_s, R_t)$
- 4: $(R_s, R_t) \leftarrow \text{decr}u(R_s, R_t)$
- 5: **end while**
- 6: $O \leftarrow O(\bar{R}_s, \bar{R}_t)$, $a \leftarrow \text{anru}(O)$
- 7: **return** $(\bar{R}_s, \bar{R}_t, O, a)$

The core intuition behind the Partition Cut (visualized in Figure 2) is to identify the smallest possible geometric region where the influence of s and t meet. Initially, spheres are grown around the terminals until they intersect. We then apply the decrement rule, decru, to systematically shrink these radii until any further reduction would result in an empty intersection.

By selecting an anchor node a within this final, minimal overlap (Definition 4.8), we effectively decompose the original $s \rightarrow t$ query into two independent $s \rightarrow a$ and $a \rightarrow t$ subproblems. These subproblems are then solved within their respective induced spherical subgraphs.

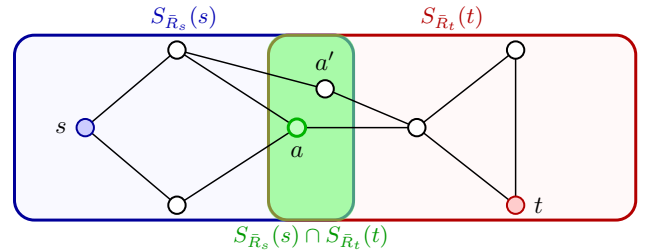


Figure 2: **Last nonempty overlap.** Blue and red spheres overlap in the green region containing both a and a' . Potential anchor node a is selected according to Definition 4.8.

A natural question is whether the Partition cut of Algorithm 1 actually preserves feasibility of the original $s \rightarrow t$ routing problem. In other words: *Does splicing the two subpaths at the chosen anchor still yield a valid global route?* The following statement makes this precise:

Proposition 4.9 (Feasibility preservation) Let $(\bar{R}_s, \bar{R}_t, O, a)$ be returned by Algorithm 1. If $P_{s \rightarrow a}$ is a feasible path in $G_{\bar{R}_s}^{\text{ind}}(s)$ and $P_{a \rightarrow t}$ is a feasible path in $G_{\bar{R}_t}^{\text{ind}}(t)$, then $P_{s \rightarrow a} \circ P_{a \rightarrow t}$ is a feasible $s \rightarrow t$ path in G .

Proof. We provide a short proof sketch: Both subgraphs are induced, hence every used edge is in G . Since $a \in O(\bar{R}_s, \bar{R}_t)$, concatenating at a yields a valid $s \rightarrow t$ path in G . \square

4.3 RECURSIVE SPHERICAL PARTITIONING

The following procedure extends the partition cut of Algorithm 1 into a recursive framework. The objective is to decompose a global $s \rightarrow t$ routing task into a collection of manageable subproblems, each strictly confined to an induced spherical subgraph where the radius does not exceed a bound R_{max} . For a comprehensive overview of all configurable parameters, please refer to Appendix A.2.

Each subproblem is formalized as a *task triple* (H, u, w) , representing a localized search from node u to node w within the induced subgraph H . We treat the resulting task set \mathcal{T} as a sequence ordered along the $s \rightarrow t$ trajectory. This ordering ensures that concatenating the locally optimal paths induces a valid global path. For simplicity, we refer to this locally optimal path as the path returned by Algorithm 2.

Algorithm 2 Recursive spherical partitioning

Require: graph $G = (V, E)$, terminals (s, t) , bound R_{max} , rules `staru`, `decru`, `anru`
Ensure: set \mathcal{T} of task triples (H, u, w)

```

1 function SPHPARTITION( $G, s, t, R_{\text{max}}$ )
2    $\mathcal{T} \leftarrow \emptyset$ , rule  $\leftarrow$  (staru, decru, anru)
3    $(R_s, R_t, O, a) \leftarrow \text{PARTCUT}(G, s, t, \text{rule})$   $\triangleright$  Alg. 1
4   if  $R_s \leq R_{\text{max}}$  then
5      $\mathcal{T} \leftarrow \mathcal{T} \cup \{(G_{R_s}^{\text{ind}}(s), s, a)\}$ 
6   else
7      $\mathcal{T} \leftarrow \mathcal{T} \cup \text{SPHPARTITION}(G_{R_s}^{\text{ind}}(s), s, a, R_{\text{max}})$ 
8   end if
9   if  $R_t \leq R_{\text{max}}$  then
10     $\mathcal{T} \leftarrow \mathcal{T} \cup \{(G_{R_t}^{\text{ind}}(t), a, t)\}$ 
11  else
12     $\mathcal{T} \leftarrow \mathcal{T} \cup \text{SPHPARTITION}(G_{R_t}^{\text{ind}}(t), a, t, R_{\text{max}})$ 
13  end if
14  return  $\mathcal{T}$ 
15 end function

```

Algorithm 2 starts by initializing the set of tasks \mathcal{T} to be empty (lines 1-3). It then performs a partition cut on the original problem (G, s, t) , which returns the radii (R_s, R_t) , the last nonempty overlap O , and an anchor $a \in O$. The anchor acts as a splitting point that separates the global $s \rightarrow t$ route into two sides.

The algorithm then branches into two recursive checks. On the s -side (lines 4-7), the relevant subproblem is

$(G_{R_s}^{\text{ind}}(s), s, a)$. If the radius R_s is already below the cap R_{max} , this subproblem is considered sufficiently small and is added to the task set \mathcal{T} . If not, the procedure calls itself recursively on this induced subgraph to split it further. Symmetrically, the t -side branch (lines 8-11) processes the subproblem $(G_{R_t}^{\text{ind}}(t), a, t)$: either it is recorded directly if $R_t \leq R_{\text{max}}$, or it is further partitioned by another recursive call.

Finally, once both branches have been processed, the algorithm returns (line 12) the accumulated set \mathcal{T} of task triples. By construction, concatenating the solutions to these recorded subproblems along their anchors yields a valid overall $s \rightarrow t$ route.

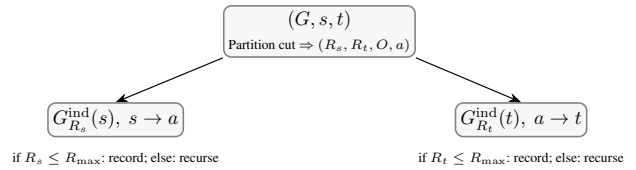


Figure 3: **Recursive splitting.** Any side above the bound is split again by Algorithm 1; leaves are independent subproblems.

Figure 3 illustrates this recursive structure. Each partition cut splits the problem into two boxes, one for the start-side and one for the target-side. If the radius on a side is within the bound, the box is recorded as a leaf; otherwise, it is expanded by another partition cut.

4.3.1 Baseline application

The recursive decomposition defined in Algorithm 2 yields a set of leaf tasks, each formalized as (H, u, w) . This process effectively reduces the high-complexity global $s \rightarrow t$ routing problem into a collection of independent, localized subproblems. Because these subproblems are spatially confined and bounded by the bound R_{max} , they are sufficiently small to be solved efficiently using standard routing methods or off-the-shelf optimizers.

Algorithm 3 Baseline application with spherical partitioning

Require: graph $G = (V, E)$, terminals (s, t) , bound R_{max} , solver `optimize`(\cdot)
Ensure: feasible route \mathcal{R}

```

1:  $\mathcal{R} \leftarrow \emptyset$ ;  $\mathcal{T} \leftarrow \text{SPHPARTITION}(G, s, t, R_{\text{max}})$ 
2: for each  $(H, u, w) \in \mathcal{T}$  do
3:    $\mathcal{R} \leftarrow \mathcal{R} \circ \text{optimize}(H, u, w)$ 
4: end for
5: return  $\mathcal{R}$ 

```

Algorithm 3 details the integration of recursive spherical partitioning into a complete routing pipeline. The procedure begins by decomposing the input graph G and terminals

(s, t) into a sequence of smaller, manageable subproblems with resulting task (H, u, w) .

Subsequently, an arbitrary downstream solver, $\text{optimize}(H, u, w)$, is applied to each subproblem to compute a local path. These local solutions are then concatenated in the order established by the partition's anchors, forming a globally valid $s \rightarrow t$ route \mathcal{R} . A critical advantage of this framework is that because the subproblems are mutually independent, they can be solved in parallel. Furthermore, the procedure remains strictly solver-agnostic, allowing the utilization of various downstream optimizer without modification to the underlying partitioning logic.

4.4 OPTIMALITY CONDITIONS

We now consider the special case of a finite, connected, undirected, and *unweighted* graph $G = (V, E)$. As before, let $d(\cdot, \cdot)$ denote the unweighted shortest-path distance, or *hop count*. Building upon the definition of the sphere $S_R(\tilde{v})$ for a node $\tilde{v} \in V$ and radius $R \in \mathbb{N}$ (Definition 4.1), we revisit the overlap $O(R_s, R_t)$ established in Definition 4.4 for a given pair of radii (R_s, R_t) .

In the following, we demonstrate that Algorithm 1, when applied to unweighted graphs using the monotone decrement rule from Example 4.6, preserves optimality. We thus provide a stronger result compared to the the general weighted setting, where Proposition 4.9 ensures the preservation of route feasibility only.

Furthermore, this result allows to compute a globally shortest path without invoking any additional optimization routines or solver-specific procedures, provided we apply the recursion until the radii are equal to 1.

We begin by formalizing the *Strong Minimality Condition*, which characterizes the minimal non-empty overlap induced by the monotone decrement rule in terms of the associated radius tuple (R_s, R_t) .

Definition 4.10 (Strong Minimality Condition) A tuple (R_s, R_t) is strongly minimal if

$$\begin{aligned} O(R_s, R_t) &\neq \emptyset, \\ O(R_s - 1, R_t) &= \emptyset, \\ O(R_s, R_t - 1) &= \emptyset. \end{aligned}$$

The next result shows by combining Definitions 4.4 and 4.10 that strong minimality forces all overlap vertices to lie simultaneously on the boundaries of both spheres determined by (R_s, R_t) .

Lemma 4.11 (Boundary property) If (R_s, R_t) is strongly minimal, then for every $v \in O(R_s, R_t)$,

$$d(s, v) = R_s \quad \text{and} \quad d(t, v) = R_t.$$

Proof. Let $v \in O(R_s, R_t)$. If $d(s, v) \leq R_s - 1$, then $v \in O(R_s - 1, R_t)$, contradicting strong minimality. Hence $d(s, v) = R_s$. The argumentation for t is analogous, yielding $d(t, v) = R_t$. \square

Having established the boundary property of strongly minimal overlaps, we now derive the key consequence of the monotone decrement rule. The following *Meet-in-the-middle equality* formalizes that a strongly minimal radius tuple satisfies

$$R_s + R_t = d(s, t),$$

thereby identifying the last overlap of two spheres.

Lemma 4.12 (Meet-in-the-middle equality) If (R_s, R_t) is strongly minimal, then

$$R_s + R_t = d(s, t).$$

Proof. Choose $a \in O(R_s, R_t)$. Since $a \in S_{R_s}(s)$ and $a \in S_{R_t}(t)$, there exists an s - t path via a of length at most $R_s + R_t$, hence $d(s, t) \leq R_s + R_t$.

Assume for contradiction that $d(s, t) \leq R_s + R_t - 1$. Let P be a shortest s - t path of length $L = d(s, t)$. Let v be the vertex on P at distance R_s from s . Since P is the shortest s - t path, then $d(s, v) = R_s$ and $d(t, v) = L - R_s \leq R_t - 1$. Thus $v \in O(R_s, R_t - 1)$ contradicts strong minimality. Therefore $d(s, t) \geq R_s + R_t$, and equality follows. \square

Lemma 4.12 constitutes the central argument of our main optimality theorem: it ensures that any anchor selected from the minimal overlap lies on a globally shortest path and thus enables recursive preservation of optimality. Note that all definitions and lemmas apply to any terminal pair (u, w) (replacing (s, t)), in every recursive subproblem.

Theorem 4.13 (Global preservation) Let $G = (V, E)$ be a finite, connected, undirected, and unweighted graph and assume that the monotone decrement rule is used. Then the concatenated s - t path returned by Algorithm 2 is a globally shortest path in G .

Proof. We argue by induction over the recursion tree:

Local optimal split. Fix any subproblem with endpoints (u, w) and a strongly minimal pair (R_u, R_w) as induced by undirected graphs and the monotone decrement rule with anchor $a \in O(R_u, R_w)$. Applying Lemma 4.11, we observe that the anchor a lies on the boundaries of both spheres, such that $d(u, a) = R_u$ and $d(a, w) = R_w$. It follows from Lemma 4.12 that these radii sum exactly to the distance between u and w , i.e. $R_u + R_w = d(u, w)$. Hence

$$d(u, a) + d(a, w) = d(u, w),$$

so a lies on a shortest u - w path and the split $(u, w) \mapsto (u, a), (a, w)$ is consistent with global optimality for that subproblem.

Inductive step. Assume recursively computed solutions are shortest for the two child subproblems (u, a) and (a, w) . Their concatenation has length $d(u, a) + d(a, w) = d(u, w)$, hence is shortest for the parent subproblem. Applying this from leaves to the root yields a globally shortest s - t path. \square

5 NUMERICAL EXPERIMENTS

Our experiments are designed to evaluate whether our method delivers significant performance gains (in terms of runtime and optimality gap) over established graph-routing baselines.

5.1 DATASET

For our empirical evaluation, we use the `West-USA-road` benchmark suite from the 9th DIMACS Implementation Challenge on Shortest Paths [Demetrescu et al., 2009]. This dataset represents real-world road networks. Nodes correspond to intersections and edges represent road segments with positive weights equal to physical length.

5.2 EXPERIMENTAL SETUP

For each problem instance p (with according instance seed), we draw a source-target pair (s, t) uniformly at random. To capture variability from the randomized anchor selection, we run five independent trials with inner seeds q for each source-target pair. We report results aggregated by the median and mean across these seeds. Further details regarding graph dimensions and seed selection are provided in Appendix A.3.

We apply Algorithm 2 with a maximum radius bound of $R_{\max} = 1800$ (see Appendix A.3 for tuning rationale). Because *SPHERE* generates independent induced subgraphs, we solve the resulting leaf tasks in parallel using Dijkstra’s algorithm and report the end-to-end wall-clock time, including the partitioning and concatenation overhead.¹

We compare *SPHERE* against an optimal reference using Dijkstra’s algorithm on the full graph, as well as Louvain and Corridor routing. Unlike *SPHERE*, these static partitioning schemes compute cuts globally rather than conditioning on the specific (s, t) query. Consequently, they cannot guarantee feasibility without boundary repair, nor do they naturally yield the mathematically independent subproblems required for the same drop-in parallel execution framework applied to our method. While static partitions could theoretically be parallelized, they often require shared boundary synchronization or global quotient graphs to ensure path consistency,

¹The graph data and implementation will be made publicly available upon the manuscript’s acceptance.

whereas *SPHERE* subproblems are self-contained by construction. (See Appendix A.3 for implementation and library details).

Let $m \in \{\text{SPHERE}, \text{CORRIDOR}, \text{LOUVAIN}\}$ denote the method. For each problem seed p and inner seed q , let $C_{p,q}^{(m)}$ be the route cost returned by m , and let C_p^* be the shortest-path cost from Dijkstra’s algorithm on the full graph for the same (s, t) . Define the relative optimality gap

$$\Delta_{p,q}^{(m)} = \frac{C_{p,q}^{(m)} - C_p^*}{C_p^*}.$$

For each p , aggregate across the five inner seeds by the median:

$$\begin{aligned} \tilde{\Delta}_p^{(m)} &= \text{median}_{q=1,\dots,5} \Delta_{p,q}^{(m)}, \\ \tilde{T}_p^{(m)} &= \text{median}_{q=1,\dots,5} T_{p,q}^{(m)}, \end{aligned}$$

where $T_{p,q}^{(m)}$ is the end-to-end wall-clock time. For completeness, we also report means:

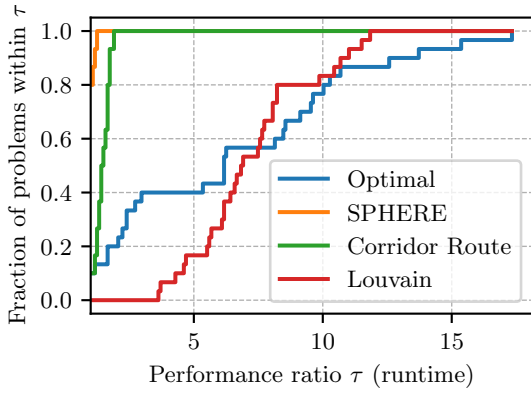
$$\bar{\Delta}_p^{(m)} = \frac{1}{5} \sum_{q=1}^5 \Delta_{p,q}^{(m)}, \quad \bar{T}_p^{(m)} = \frac{1}{5} \sum_{q=1}^5 T_{p,q}^{(m)}.$$

5.3 RESULTS

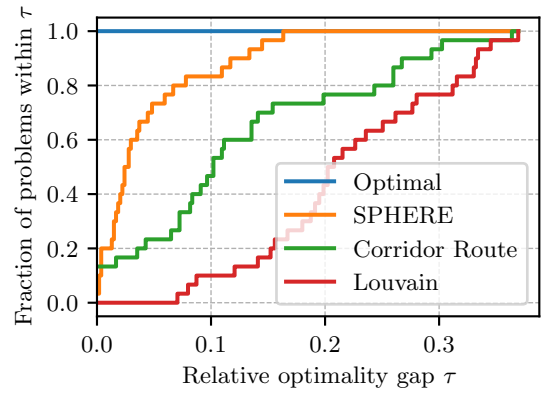
Across 30 West-USA instances with five inner seeds each, *SPHERE* achieves faster end-to-end runtimes than the three baselines and matches near-optimal route quality. We use performance and accuracy profiles for visualization [Dolan and Moré, 2002, Beiranvand et al., 2017]. Both are computed per instance from the median over seeds. Mean-based profiles for runtime and accuracy are presented as well.

Figures 4a and 4c plot the fraction of instances solved within a performance ratio τ of the best method on that instance. *SPHERE*’s curve lies above the Louvain and corridor routes for most τ , indicating uniformly stronger or equal runtime across instances. Interestingly, for small τ , Louvain’s curve lies below Dijkstra’s, despite being a suboptimal method. However, at larger τ it crosses and stays above, indicating tail slowdowns for Dijkstra. This suggests that *SPHERE* not only improves median runtime, but also avoids the heavy-tailed slowdowns observed in both Dijkstra and Louvain, resulting in tighter runtime distributions and fewer extreme outliers, which makes *SPHERE*’s runtimes more predictable across different instances.

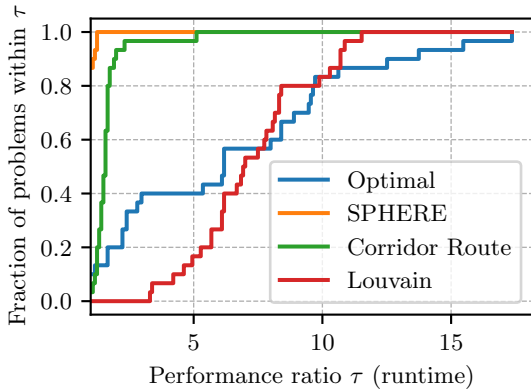
Figures 4b and 4d report the fraction of instances whose relative optimality gap is at most τ . Dijkstra attains zero gap by construction. *SPHERE*’s curve dominates the partition baselines across τ , yielding smaller or equal gaps on the majority of instances. This confirms that cutting inside the s - t overlap and solving on induced spheres preserves high-quality routes without boundary repair.



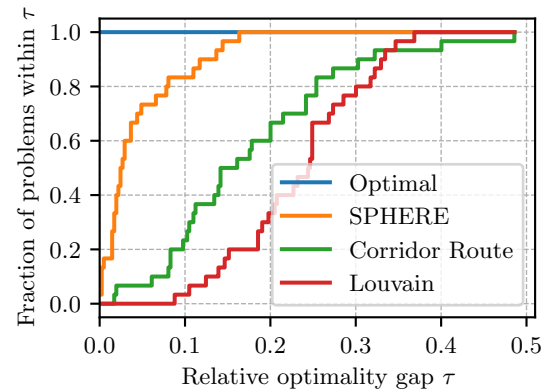
(a) Runtime profile based on the **median** over five seeds



(b) Accuracy profile based on the **median** over five seeds



(c) Runtime profile based on the **mean** over five seeds



(d) Accuracy profile based on the **mean** over five seeds

Figure 4: Performance and accuracy profiles of 30 instances based on median and mean over five seeds.

Against the partition baselines (Louvain and METIS corridor), *SPHERE* Pareto-dominates on 26 of 30 instances in terms of average metrics. It is both faster and has a smaller optimality gap (Appendix A.4). The remaining three show a speed-quality trade-off where *SPHERE* is not dominated by another algorithm. In other words, *SPHERE* consistently lies on or close to the empirical speed-quality frontier, while Louvain and corridor-routing often face a trade-off between being faster but less accurate, or more accurate but substantially slower.

Repeating the analysis with means over seeds yields profiles that do not differ materially from the median-based plots, supporting robustness to the randomized anchor selection. Additionally, the full results in Appendix A.4 show low dispersion across seeds. The results indicate reliability across varying query geometries and suggest that spherical decomposition effectively captures the core topological features necessary for high-quality routing, regardless of internal stochasticity. For *SPHERE*, the optimality-gap standard deviation is 0 on 16 instances and is the lowest among all methods on all but one instance. For further information, we refer to Appendix A.4.

6 CONCLUSION AND OUTLOOK

We introduced *SPHERE*, a routing scheme that splits an $s-t$ query by cutting *inside* the last nonempty overlap of hop-spheres around s and t . This placement preserves feasibility without boundary repair, confines each side to an induced subgraph, and allows the subproblems to be solved independently with standard shortest-path routines and in parallel. On million-scale road networks, *SPHERE* achieves faster runtimes and smaller optimality gaps than state-of-the-art static and community-based partitioning methods. Notably, our approach eliminates the heavy-tail runtime outliers common in exact solvers, providing high statistical stability across randomized anchor selections.

Future work will explore data-driven anchor selection to further improve robustness across diverse graph topologies. Additionally, *SPHERE* can serve as a wrapper for complex neural combinatorial optimizers that typically struggle with large-scale instances. Another direction could be to automate the tuning of the radius cap R_{\max} to adaptively balance computational budgets against query complexity. These advancements will maintain *SPHERE*'s simplicity and parallelism while further enhancing speed and stability.

References

- Hannah Bast, Daniel Delling, Andrew Goldberg, Matthias Müller-Hannemann, Thomas Pajor, Peter Sanders, Dorothea Wagner, and Renato F. Werneck. *Route Planning in Transportation Networks*, pages 19–80. Springer International Publishing, Cham, 2016. ISBN 978-3-319-49487-6. doi: 10.1007/978-3-319-49487-6_2. URL https://doi.org/10.1007/978-3-319-49487-6_2.
- Vahid Beiranvand, Warren Hare, and Yves Lucet. Best practices for comparing optimization algorithms. *Optimization and Engineering*, 18(4):815–848, 2017. doi: 10.1007/s11081-017-9366-1. URL <https://doi.org/10.1007/s11081-017-9366-1>.
- Vincent D Blondel, Jean-Loup Guillaume, Renaud Lambiotte, and Etienne Lefebvre. Fast unfolding of communities in large networks. *Journal of Statistical Mechanics: Theory and Experiment*, 2008(10):P10008, oct 2008. doi: 10.1088/1742-5468/2008/10/P10008. URL <https://doi.org/10.1088/1742-5468/2008/10/P10008>.
- Camil Demetrescu, Andrew V. Goldberg, and David S. Johnson, editors. *The Shortest Path Problem: Ninth DIMACS Implementation Challenge*, volume 74 of *DIMACS Series in Discrete Mathematics and Theoretical Computer Science*. American Mathematical Society, Providence, RI, 2009. ISBN 978-0-8218-4383-3. doi: 10.1090/dimacs/074. URL <https://doi.org/10.1090/dimacs/074>.
- E. W. Dijkstra. A note on two problems in connexion with graphs. *Numerische Mathematik*, 1(1):269–271, 1959. doi: 10.1007/BF01386390. URL <https://doi.org/10.1007/BF01386390>.
- Elizabeth D. Dolan and Jorge J. Moré. Benchmarking optimization software with performance profiles. *Mathematical Programming*, 91(2):201–213, 2002. doi: 10.1007/s101070100263. URL <https://doi.org/10.1007/s101070100263>.
- Dominique Feillet, Pierre Dejax, Michel Gendreau, and Cyrille Gueguen. An exact algorithm for the elementary shortest path problem with resource constraints: Application to some vehicle routing problems. *Networks*, 44(3):216–229, 2004. doi: <https://doi.org/10.1002/net.20033>. URL <https://onlinelibrary.wiley.com/doi/abs/10.1002/net.20033>.
- Refael Hassin. Approximation schemes for the restricted shortest path problem. *Mathematics of Operations Research*, 17(1):36–42, 1992. doi: 10.1287/moor.17.1.36. URL <https://doi.org/10.1287/moor.17.1.36>.
- Robert Holte, Ariel Felner, Guni Sharon, and Nathan Sturtevant. Bidirectional search that is guaranteed to meet in the middle. *Proceedings of the AAAI Conference on Artificial Intelligence*, 30(1), Mar. 2016. doi: 10.1609/aaai.v30i1.10436. URL <https://ojs.aaai.org/index.php/AAAI/article/view/10436>.
- Stefan Irnich and Guy Desaulniers. *Shortest Path Problems with Resource Constraints*, pages 33–65. Springer US, Boston, MA, 2005. ISBN 978-0-387-25486-9. doi: 10.1007/0-387-25486-2_2. URL https://doi.org/10.1007/0-387-25486-2_2.
- Hermann Kaindl and Gerhard Kainz. Bidirectional heuristic search reconsidered. *Journal of Artificial Intelligence Research*, 7:283–317, 1997. doi: 10.1613/jair.460.
- George Karypis and Vipin Kumar. A fast and high quality multilevel scheme for partitioning irregular graphs. *SIAM Journal on Scientific Computing*, 20(1):359–392, 1998. doi: 10.1137/S1064827595287997. URL <https://doi.org/10.1137/S1064827595287997>.
- B. W. Kernighan and S. Lin. An efficient heuristic procedure for partitioning graphs. *The Bell System Technical Journal*, 49(2):291–307, Feb 1970. ISSN 0005-8580. doi: 10.1002/j.1538-7305.1970.tb01770.x.
- Yeong-Dae Kwon, Jinho Choo, Byoungjip Kim, Iljoo Yoon, Youngjune Gwon, and Seungjai Min. Pomo: policy optimization with multiple optima for reinforcement learning. In *Proceedings of the 34th International Conference on Neural Information Processing Systems, NIPS '20*, Red Hook, NY, USA, 2020. Curran Associates Inc. ISBN 9781713829546.
- T. A. J. Nicholson. Finding the shortest route between two points in a network. *The Computer Journal*, 9(3):275–280, 11 1966. ISSN 0010-4620. doi: 10.1093/comjnl/9.3.275. URL <https://doi.org/10.1093/comjnl/9.3.275>.
- David Pisinger and Stefan Ropke. A general heuristic for vehicle routing problems. *Computers & Operations Research*, 34(8):2403–2435, 2007. ISSN 0305-0548. doi: <https://doi.org/10.1016/j.cor.2005.09.012>. URL <https://www.sciencedirect.com/science/article/pii/S0305054805003023>.
- Ira Pohl. Bi-directional and heuristic search in path problems. Technical Report SLAC-104, Stanford Linear Accelerator Center, Stanford, CA, 1969. URL <https://www.slac.stanford.edu/pubs/slacreports/reports04/slac-r-104.pdf>.
- Václav Rozhoň, Bernhard Haeupler, Anders Martinsson, Christoph Grunau, and Goran Zuzic. Parallel breadth-first search and exact shortest paths and stronger notions for approximate distances. In *Proceedings of the 55th*

Annual ACM Symposium on Theory of Computing, STOC 2023, page 321–334, New York, NY, USA, 2023. Association for Computing Machinery. ISBN 9781450399135. doi: 10.1145/3564246.3585235. URL <https://doi.org/10.1145/3564246.3585235>.

Jianbo Shi and J. Malik. Normalized cuts and image segmentation. *IEEE Transactions on Pattern Analysis and Machine Intelligence*, 22(8):888–905, Aug 2000. ISSN 1939-3539. doi: 10.1109/34.868688.

Thibaut Vidal. Hybrid genetic search for the CVRP: Open-source implementation and swap* neighborhood. *Computers & Operations Research*, 140:105643, 2022. ISSN 0305-0548. doi: <https://doi.org/10.1016/j.cor.2021.105643>. URL <https://www.sciencedirect.com/science/article/pii/S030505482100349X>.

Jianan Zhou, Zhiguang Cao, Yaoxin Wu, Wen Song, Yining Ma, Jie Zhang, and Chi Xu. Mvmoe: Multi-task vehicle routing solver with mixture-of-experts, 2024. URL <https://arxiv.org/abs/2405.01029>.

A APPENDIX

A.1 NOTATION

Table 1: Notation

Symbol	Description
$V = \{1, \dots, m\}$	Node (vertex) index set.
$\mathcal{P}(V)$	Power set of V .
$E \subseteq V \times V$	Edge set; undirected unless stated.
$G = (V, E)$	Graph with node set V and edge set E .
$d_G(u, v)$	Shortest unweighted path distance on G .
$G[U]$	Induced subgraph on node set U .
$S_R(\tilde{v}) = \{v \in V : d_G(\tilde{v}, v) \leq R\}$	(Closed) hop sphere (ball) of radius R around \tilde{v} .
$S_s(r) \equiv S_r(s), S_t(r) \equiv S_r(t)$	Shorthand spheres around s and t .
$O(R_s, R_t) = S_{R_s}(s) \cap S_{R_t}(t)$	Overlap of the two spheres.

Continued on next page

Table 1: Notation (Continued)

Symbol	Description
$V = \{1, \dots, m\}$	Node (vertex) index set.
$a \in V, S^\dagger \subseteq O(R_s, R_t)$	Anchor node; optional candidate anchor set.
$G_s = G[S_{R_s}(s)], G_t = G[S_{R_t}(t)]$	Induced subgraphs around s and t at radii R_s, R_t .
$(H, u, w), \mathcal{T}$	Task triple “route $u \rightarrow w$ inside H ”; set of leaf tasks.
$ X $	Cardinality of a (finite) set X .

A.2 PARAMETERS

Table 2: Parameters

Symbol	Description
$R_{\max} \in \mathbb{N}$	Maximum allowed radius for spherical subgraphs (controls subproblem diameter).
$V_{\max} \in \mathbb{N}, E_{\max} \in \mathbb{N}$	Optional caps on nodes/edges permitted in any subgraph $G[U]$.
$\varepsilon_{\text{overlap}} \in \mathbb{N}_0$	Minimum required overlap size (require $ O(R_s, R_t) \geq \varepsilon_{\text{overlap}}$).
$\Delta r \in \mathbb{N}$	Radius increment/decrement step during sphere growth/shrinking (if using fixed steps; typically $\Delta r = 1$).
$L_{\max} \in \mathbb{N}$	Maximum recursion depth for repeated splits.
$k_{\text{anchor}} \in \mathbb{N}$	Number of anchors to select from O (often $k_{\text{anchor}} = 1$).

A.3 IMPLEMENTATION DETAILS AND HYPERPARAMETERS

Graph Dimensions. The `West-USA-road` network consists of 6, 262, 104 nodes and 15, 248, 146 edges. The large scale of this network makes it a challenging benchmark for standard exact solvers.

Instance and Seed Selection. The 30 problem instances p are defined by fixed global seeds to ensure reproducibility

of the (s, t) pairs. For each p , 5 inner seeds q control the stochasticity of the anru function in Algorithm 1.

Radius bound (R_{\max}). The tunable bound R_{\max} controls the maximum diameter of the subproblems generated by Algorithm 3. Throughout development, we established a robust rule of thumb: when routing within a spherical subgraph of hop radius R , choosing $R_{\max} \in [R/2, R/1.7]$ delivers high-quality solutions at both low computational cost and effort. For the West-USA benchmark instances, a single sphere with $R \approx 3200$ generally covers the necessary region. Thus, our chosen bound of $R_{\max} = 1800$ lies squarely in this optimal band, carefully balancing the likelihood of an s - t overlap against the complexity of the resulting leaf tasks.

Baseline Configurations. The baseline pipelines were implemented using standard libraries to ensure a fair comparison. The corridor-routing baseline utilizes `PyMetis` to compute the initial $k = 64$ cell partition. The Louvain community-detection baseline was run using its default modularity-optimization parameters, seeded where applicable to ensure deterministic execution. It is worth noting that because these static partitioning schemes compute cuts globally rather than conditioning on the specific (s, t) query, they cannot guarantee feasibility without boundary repair, nor do they yield strictly independent leaves suitable for the same parallel execution framework applied to *SPHERE*.

A.4 PERFORMANCE PER INSTANCE

Continued on next page.

Table 3: WestUSA – Routing

		avg compute time	avg opt. gap	median opt. gap	std opt. gap
P1	<i>SPHERE</i>	135.73	0.08	0.06	0.02
	Corridor Route	173.97	0.24	0.07	0.36
	Louvain	1047.77	0.25	0.28	0.05
P2	<i>SPHERE</i>	138.27	0.12	0.12	0.00
	Corridor Route	187.87	0.14	0.09	0.16
	Louvain	1072.17	0.34	0.35	0.05
P3	<i>SPHERE</i>	165.25	0.03	0.03	0.00
	Corridor Route	190.12	0.08	0.10	0.06
	Louvain	1130.18	0.18	0.18	0.05
P4	<i>SPHERE</i>	370.06	0.11	0.11	0.00
	Corridor Route	574.18	0.25	0.26	0.10
	Louvain	1230.71	0.37	0.37	0.03
P5	<i>SPHERE</i>	126.88	0.05	0.05	0.00
	Corridor Route	171.35	0.10	0.11	0.06
	Louvain	1129.89	0.14	0.14	0.06
P6	<i>SPHERE</i>	301.07	0.02	0.03	0.00
	Corridor Route	571.56	0.18	0.15	0.14
	Louvain	1265.49	0.25	0.20	0.12
P7	<i>SPHERE</i>	213.59	0.00	0.00	0.00
	Corridor Route	354.04	0.27	0.36	0.17
	Louvain	1197.91	0.32	0.32	0.04
P8	<i>SPHERE</i>	157.02	0.01	0.01	0.00
	Corridor Route	224.89	0.32	0.27	0.16
	Louvain	1165.53	0.09	0.07	0.03
P9	<i>SPHERE</i>	390.68	0.02	0.02	0.00
	Corridor Route	396.99	0.13	0.10	0.10
	Louvain	1274.68	0.23	0.21	0.06
P10	<i>SPHERE</i>	137.20	0.02	0.02	0.00
	Corridor Route	197.31	0.02	0.00	0.03
	Louvain	1141.72	0.27	0.33	0.10
P11	<i>SPHERE</i>	130.96	0.13	0.13	0.01
	Corridor Route	167.76	0.20	0.07	0.24
	Louvain	1057.36	0.33	0.33	0.00
P12	<i>SPHERE</i>	264.38	0.04	0.04	0.00
	Corridor Route	234.53	0.24	0.20	0.13
	Louvain	1160.17	0.25	0.17	0.13
P13	<i>SPHERE</i>	123.22	0.00	0.00	0.00
	Corridor Route	200.92	0.10	0.00	0.16
	Louvain	1308.92	0.18	0.19	0.03
P14	<i>SPHERE</i>	234.34	0.14	0.14	0.00
	Corridor Route	358.43	0.25	0.24	0.17
	Louvain	1414.78	0.33	0.31	0.05
P15	<i>SPHERE</i>	211.37	0.00	0.00	0.00
	Corridor Route	300.88	0.11	0.10	0.09
	Louvain	1288.33	0.15	0.15	0.02

Continued on next page

		avg compute time	avg opt. gap	median opt. gap	std opt. gap
	<i>SPHERE</i>	136.40	0.04	0.04	0.00
P16	Corridor Route	221.84	0.08	0.02	0.13
	Louvain	1400.16	0.20	0.19	0.05
	<i>SPHERE</i>	119.90	0.01	0.00	0.02
P17	Corridor Route	193.90	0.02	0.00	0.03
	Louvain	1266.58	0.20	0.21	0.07
	<i>SPHERE</i>	123.18	0.08	0.08	0.01
P18	Corridor Route	205.16	0.06	0.00	0.07
	Louvain	1409.96	0.32	0.33	0.03
	<i>SPHERE</i>	205.97	0.02	0.02	0.00
P19	Corridor Route	1052.15	0.40	0.30	0.31
	Louvain	1401.55	0.25	0.25	0.05
	<i>SPHERE</i>	170.12	0.00	0.00	0.00
P20	Corridor Route	391.16	0.30	0.08	0.34
	Louvain	1414.17	0.10	0.08	0.04
	<i>SPHERE</i>	326.25	0.01	0.01	0.00
P21	Corridor Route	506.65	0.20	0.14	0.12
	Louvain	1502.53	0.30	0.22	0.16
	<i>SPHERE</i>	137.27	0.03	0.03	0.00
P22	Corridor Route	180.60	0.49	0.29	0.51
	Louvain	1135.72	0.28	0.26	0.08
	<i>SPHERE</i>	172.50	0.01	0.01	0.00
P23	Corridor Route	211.28	0.08	0.04	0.11
	Louvain	1065.85	0.21	0.20	0.06
	<i>SPHERE</i>	145.29	0.02	0.02	0.00
P24	Corridor Route	202.11	0.21	0.26	0.13
	Louvain	1009.77	0.27	0.28	0.07
	<i>SPHERE</i>	160.44	0.02	0.02	0.00
P25	Corridor Route	219.89	0.11	0.04	0.14
	Louvain	1059.09	0.12	0.12	0.02
	<i>SPHERE</i>	172.71	0.03	0.03	0.00
P26	Corridor Route	203.42	0.17	0.13	0.14
	Louvain	1054.63	0.24	0.19	0.13
	<i>SPHERE</i>	246.94	0.02	0.02	0.00
P27	Corridor Route	479.93	0.14	0.06	0.11
	Louvain	1388.28	0.22	0.20	0.04
	<i>SPHERE</i>	159.42	0.00	0.00	0.00
P28	Corridor Route	267.58	0.16	0.13	0.17
	Louvain	1274.86	0.19	0.16	0.08
	<i>SPHERE</i>	232.46	0.07	0.07	0.00
P29	Corridor Route	354.39	0.14	0.11	0.07
	Louvain	1219.90	0.25	0.24	0.03
	<i>SPHERE</i>	142.64	0.16	0.16	0.00
P30	Corridor Route	175.93	0.10	0.08	0.10
	Louvain	1162.54	0.15	0.09	0.10